МАГНИТНАЯ ГИДРОДИНАМИКА. — 1995. — Т.31, № 1. — С. 3 — 18

A. C. Neubrand, J.-P. Garandet

Commissariat à l'Energie Atomique DTA/CEREM/SES - Centre d'Etudes Nucléaires de Grenoble - 17, av. des Martyrs - 38054 Grenoble Cedex 9 - France

R. Moreau and T. Alboussière

EPM MADYLAM - CNRS UPR A 9033 - ENSHMG - BP 95 - 38402 St Martin d'Hères Cedex - France

EFFECT OF A SLIGHT NON-UNIFORMITY OF THE MAGNETIC FIELD ON MHD CONVECTION

А. К. Нойбранд, Ж.-П. Жарандэ, Р. Моро, Т. Албуссьер

ВЛИЯНИЕ СЛАБОЙ НЕОДНОРОДНОСТИ МАГНИТНОГО ПОЛЯ НА МАГНИТОГИДРОДИНАМИЧЕСКУЮ КОНВЕКЦИЮ

Изучена чувствительность МГД конвекции по отношению к слабой неоднородности магнитного поля. Работа представляет собой дальнейшее развитие асимптотического анализа процессов при больших числах Гартмана, проведенного в [1] для случая однородного постоянного вертикального магнитного поля. Неоднородность магнитного поля **b** предполагается намного меньше однородного магнитного поля нулевого порядка $\mathbf{B}_0$, $\lambda = b/B_0 << 1$. Далее с допущением, что обусловленные этой неоднородностью изменения скорости также малы по сравнению с решением при однородном поле, проведен анализ возмущений первого порядка. Если рабочий объем имеет идеально проводящие стенки, то изменение скорости оказывается того же порядка интенсивности, что и у магнитного поля, т.е. в относительных единицах равным λ. Но при непроводящих стенках слабая неоднородность магнитного поля может вызвать возмущение скорости порядка λHa. Этот результат может иметь серьезные последствия для приложений; например, в отношении горизонтального выращивания кристаллов по Бриджмену требования к размерам, конструкции и совершенству магнита могут оказаться намного строже, чем предполагалось до сих пор.

1. Introduction. Convection is an important phenomenon in crystal growth from the melt, as it is responsible for most of the crystal defects, such as macrosegregations and striations [2]. Two methods exist in order to reduce these liquid motions: the microgravity environment that reduces the buoyancy driving force, or the use of a steady magnetic field that damps the fluid flow via the electromagnetic force [3 – 5]. In all cases, it is important to understand and to predict how the applied magnetic field changes the fluid flow and affects the solute transport through the fluid and across the solid–liquid interface. The transport phenomenon can be handled with numerical as well as an order of magnitude analysis (for an application in non-MHD flows, see for instance [6]). In two former papers, a first analysis of such convective MHD flows is proposed where the magnetic field is uniform. An analytical exact solution has been obtained [7] for an idealized two-dimensionnal problem. The asymptotic analysis in [1] limited to conditions where the Hartmann number is much larger than unit, takes into account the cross-section shape and shows that the crucible geometry has a great influence on the velocity distribution: the velocity scales with GrHa^{-2} (Gr and Ha are respectively the Grashof and Hartmann numbers) when the cross-section shape is symmetric with respect to the horizontal mid plane, but may be of the order

of $GrHa^{-1}$ when the cross-section does not meet this symmetry requirement. This means that the flow is extremely sensitive to the experimental conditions and one can wonder about the required accuracy for other parameters such as the thermal gradient or the magnetic field uniformity. In this paper, we propose a first answer to this important question from an analysis of the influence of a weak non-uniformity of the magnetic field.

MHD pressure-driven flows in the presence of a non-uniform magnetic field have been studied in many papers (see for instance [8. – P. 150 – 164]). Kulikovskii [9] generalizes some results on flows in a uniform magnetic field to non-uniform magnetic field. In his core solution, singularities are put in evidence, associated with discontinuities of the quantities specifying the boundary conditions at the walls. Focusing on fully established flows at high Hartmann numbers, Todd's paper [10] is limited to circular ducts with non-uniform transverse magnetic field, and Alemany and Moreau [11] further restrict the problem to the case of a transverse multipolar magnetic field, whose axis of symmetry coincides with the duct axis. Todd shows that, in some particular cases, the strong non-uniformity of the electromagnetic resistance to the flow may yield negative velocity in part of the core. Alemany and Moreau find similar results and show that, when the number of pole pairs is larger than one, high positive velocities are located in the shear layers (where the magnetic field and the current density become parallel) or in axial jets (since the magnetic field is zero along the axis). Concerning buoyancy driven or rotational flows with non-uniform magnetic field, the studies are much rarer and only concern Czochralsky crystal growth. The effects of the so-called "cusped" magnetic field (a quadripole field) are outlined by Series and Hurle [12] and Hirata and Hoshikawa [13, 14] with the purpose to match the magnetic field to the streamlines in the melt so as to damp the convective turbulence and retain beneficial flow patterns. For application purposes, the expected role of such a magnetic field is only to suppress the solute striations.

In a Bridgman furnace, the first role assigned to the applied magnetic field is to slow down the convective mean flow (it is expected that turbulence would be damped out *a fortiori*) and to force an almost purely diffusive mass transport regime. Then, a uniform magnetic field seems to be the best candidate. This magnetic field could be generated by either a permanent magnet or an electromagnet whose polar pieces should be plane and parallel. The whole Bridgman furnace, which surrounds the crucible and the sample, should be located in the gap between these pole pieces. It is then clear that the necessary uniformity degree of the magnetic field is one of the main requirements for the magnet design, as it determines its volume and weight. Addressing this question is very different from studying the flow in the presence of a strongly non-uniform magnetic field and suggests to use a regular perturbation technique. To the zeroth order, the magnetic field $\mathbf{B}_0$ is perfectly uniform and the fluid flow is already known. We develop a first order analysis and predict the amplitude and the distribution of the disturbance of each quantity, namely the fluid velocity and current density, due to a weak magnetic field non-uniformity $\mathbf{b}$ superposed to $\mathbf{B}_0$. This greatly simplifies the problem since no discontinuities or singularities appear in the study which therefore only considers the core flow and the Hartmann layers (side layers are not taken into account). It is important to notice that this non-uniformity has nothing to do with the induced magnetic field, often called $\mathbf{b}$ too, which

is assumed to be negligible here: $Rm << \lambda << 1$, where Rm is the magnetic Reynolds number and $\lambda = b/B_0$ is the non-uniformity order of magnitude.

In section 2, we approach the problem in a general way: we assume that the unperturbed velocity and current density are known and derive the governing perturbation equations. We use the modified Elsasser variables for the perturbed quantities: $\mathbf{m}^{\pm} = \mathrm{rot}\,\mathbf{u} \pm Ha\,\mathbf{j}$ ($\mathbf{u}$ and $\mathbf{j}$ being the velocity field and current density perturbations), and we obtain a system of equations similar to that derived in [1] but with a more complex source term. The general form of the solution in the core and in the Hartmann layers is presented in sect. 3. Finally, in sect. 4, we apply it to the particular case of a horizontal Bridgman configuration with a symmetric crucible; an interesting symmetry property of the magnetic field non-uniformity is emphasized.

2. Governing equations. We consider an electrically conducting fluid contained in a cavity of a typical length-scale H in the presence of a uniform steady vertical magnetic field $\mathbf{B}_0$. We assume that:

- the physical properties of the fluid are uniform,
- the magnetic Reynolds number $Rm = \mu\sigma u H$ is very small compared to unit, so that the magnetic field is not perturbed by the flow (here, u stands for the velocity scale and μ, σ for the magnetic permeability and the electric conductivity),
- the fluid flow is steady,
- inertia is negligible,
- body forces, other than electromagnetic, are known in the whole cavity and independent of the velocity field,
- the Hartmann number $Ha = (\sigma/\rho\nu)^{1/2} B_0 H$ is large compared to unit, so that the viscous stresses are negligible in the core (ρ and ν are the density and the kinematic viscosity).

We consider that the flow in the presence of the uniform magnetic field has been determined, $\mathbf{U}_B$ being the velocity and $\mathbf{J}_B$ the current density, and we now superpose to $\mathbf{B}_0$ a slightly non-uniform disturbance $\mathbf{b}$: $\mathbf{B} = \mathbf{B}_0 + \mathbf{b}$ with $\lambda = b/B_0 << 1$ ($\mathrm{div}\,\mathbf{b} = 0$; $\mathrm{rot}\,\mathbf{b} = 0$). Our purpose is to determine $\mathbf{u}$ and $\mathbf{j}$, the velocity and current density perturbations due to the slight non-uniformity of the magnetic field, writing $\mathbf{U} = \mathbf{U}_B + \mathbf{u}$, $\mathbf{J} = \mathbf{J}_B + \mathbf{j}$ and assuming $u/U_B << 1$ and $j/J_B << 1$.

The problem is governed by the following equations (conservation of mass and electric charge, Navier – Stokes equation and Ohm's law):

$$\mathrm{div}\,\mathbf{U} = 0, \quad \mathrm{div}\,\mathbf{J} = 0, \qquad (1),(2)$$

$$-\mathrm{grad}P + \rho\mathbf{f} + \mathbf{J}\times\mathbf{B} + \rho\nu\Delta\mathbf{U} = 0\,, \quad \mathbf{J} = \sigma(-\mathrm{grad}\Phi + \mathbf{U}\times\mathbf{B}) \qquad (3),(4)$$

where $P = P_B + p$ and $\Phi = \Phi_B + \varphi$ are pressure and electric potential and $\mathbf{J}\times\mathbf{B}$ denotes the density of electromagnetic force and $\rho\mathbf{f}$ of other body forces.

The undisturbed flow is governed by the same equations with $\mathbf{B}_0$ instead of $\mathbf{B}$. Therefore, by taking their differences, we get equations for the perturbations $\mathbf{u}$, $\mathbf{j}$, p and φ of the order λ:

$$\mathrm{div}\,\mathbf{u} = 0, \quad \mathrm{div}\,\mathbf{j} = 0, \qquad (1a),(2a)$$

$$-\mathrm{grad}\,p + \mathbf{J}_B\times\mathbf{b} + \mathbf{j}\times\mathbf{B}_0 + \rho\nu\Delta\mathbf{u} = 0\,, \qquad (3a)$$

$$\mathbf{j} = \sigma(-\mathrm{grad}\,\varphi + \mathbf{U}_B\times\mathbf{b} + \mathbf{u}\times\mathbf{B}_0). \qquad (4a)$$

Since we focus on $\mathbf{u}$ and $\mathbf{j}$, we eliminate p and φ by taking rot of (3a) and (4a). Of course, p and φ could be found using the divergence of (3a) and (4a) once $\mathbf{u}$ and $\mathbf{j}$ have been determined.

Let us now use the following non-dimensional variables:

$$x = Hx^* \ , \ \mathbf{u} = \mathbf{u}^* \nu / H \ , \ \mathbf{j} = \mathbf{j}^* \nu\sigma B_0 / H \ , \ \varphi = \varphi^* \nu B_0 \ , \ \mathbf{b} = B_0 \mathbf{b}^* , \ \mathbf{B}_0 = B_0 \mathbf{e}_B$$

where the asterisk denotes a non-dimensional variable; in the following, all quantities are non-dimensional, and the asterisk is omitted. Then the set of equations (1a) – (4a) becomes:

$$\operatorname{div} \mathbf{u} = 0, \ \operatorname{div} \mathbf{j} = 0, \tag{5),(6}$$

$$\mathrm{Ha}^2 (\mathbf{e}_B \nabla)\mathbf{j} + \Delta(\operatorname{rot} \mathbf{u}) = -\mathrm{Ha}^2 \operatorname{rot}(\mathbf{J}_B \times \mathbf{b}), \tag{7}$$

$$\operatorname{rot} \mathbf{j} = \operatorname{rot}(\mathbf{U}_B \times \mathbf{b}) + (\mathbf{e}_B \nabla)\mathbf{u} \ , \ \mathbf{j} = -\operatorname{grad} \varphi + \mathbf{U}_B \times \mathbf{b} + \mathbf{u} \times \mathbf{e}_B . \tag{8),(9}$$

The modified Elsasser variables,

$$\mathbf{m}^+ = \operatorname{rot} \mathbf{u} + \mathrm{Ha}\, \mathbf{j} \ , \ \mathbf{m}^- = \operatorname{rot} \mathbf{u} - \mathrm{Ha}\, \mathbf{j}, \tag{10),(11}$$

are now introduced. Taking the rot of (8), we get:

$$(\mathbf{e}_B \nabla) \operatorname{rot} \mathbf{u} + \Delta \mathbf{j} = - \operatorname{rot} \operatorname{rot}(\mathbf{U}_B \times \mathbf{b}), \tag{12}$$

so that the equations for $\mathbf{m}^+$ and $\mathbf{m}^-$ are easily derived from the combinations (7) ± (12) the latter being multiplied by Ha:

$$\Delta \mathbf{m}^+ + \mathrm{Ha}(\mathbf{e}_B \nabla)\mathbf{m}^+ = \mathrm{Ha}\left\{\operatorname{rot}\left[\mathbf{U}_B ; \mathbf{b}\right] + \mathrm{Ha}\left[\mathbf{J}_B ; \mathbf{b}\right]\right\}, \tag{13}$$

$$\Delta \mathbf{m}^- - \mathrm{Ha}(\mathbf{e}_B \nabla)\mathbf{m}^- = -\mathrm{Ha}\left\{\operatorname{rot}\left[\mathbf{U}_B ; \mathbf{b}\right] - \mathrm{Ha}\left[\mathbf{J}_B ; \mathbf{b}\right]\right\}. \tag{14}$$

In equations (13) and (14), we used a notation

$$\left[\mathbf{a} ; \mathbf{b}\right] = -\operatorname{rot}(\mathbf{a} \times \mathbf{b}) = (\mathbf{a}\nabla)\mathbf{b} - (\mathbf{b}\nabla)\mathbf{a}$$

since $\operatorname{div} \mathbf{a} = \operatorname{div} \mathbf{b} = 0$. The system of equations still needs to be completed by relations (15), (16) which allow to come back to velocity and current density, and by the conservation equations for $\mathbf{m}^+$ and $\mathbf{m}^-$:

$$\mathbf{j} = \left(\mathbf{m}^+ - \mathbf{m}^-\right) / 2\mathrm{Ha}, \ \operatorname{rot} \mathbf{u} = \left(\mathbf{m}^+ + \mathbf{m}^-\right) / 2, \tag{15),(16}$$

$$\operatorname{div} \mathbf{m}^+ = \operatorname{div} \mathbf{m}^- = 0. \tag{17}$$

The modified Elsasser variables $\mathbf{m}^+$ and $\mathbf{m}^-$ have the property, previously found by Shercliff [15] for the non-modified Elsasser variables in pressure-driven duct flows, that each variable has no Hartmann layer on one side. The only difference between equations (13) and (14) and the equations for the unperturbed variables $\mathbf{M}^+$ and $\mathbf{M}^-$ arises from the expression in the right-hand side, which in [1] is reduced to $\mathbf{C}$, the rot of the given body forces. In our case, the right-hand side is again a given source term since $\mathbf{U}_B$ and $\mathbf{J}_B$ are known and $\mathbf{b}$ is *a priori* given, but it is more complex. Indeed, this source term contains two parts whose characteristic effects and properties are worth being distinguished. The second part $\mathrm{Ha}^2 [\mathbf{J}_B ; \mathbf{b}]$ is the driving torque density due to the electromagnetic force $\mathbf{J}_B \times \mathbf{b}$, and the first part $\pm \mathrm{Ha} \operatorname{rot}[\mathbf{U}_B ; \mathbf{b}]$ comes from the induced current density which interacts with the uniform magnetic field to give the electromagnetic force $-(\mathbf{b}\, \mathbf{e}_B)\mathbf{U}_B$, but the main point is that in the core regions where the derivatives are of the order of unit, this term is negligible with respect to $\mathrm{Ha}^2 [\mathbf{J}_B ; \mathbf{b}]$, if we assume that $\mathbf{U}_B$ and $\mathbf{J}_B$ are of the same order of magnitude. In the Hartmann layers, however, both terms are of the same order of magnitude.

3. General form of the asymptotic solutions. In the high Hartmann number limit, it is useful to distinguish different regions where the general system can be simplified: inviscid core regions where the typical length-scale is unit; and the boundary layers where it is much smaller. These layers are of

two kinds: 1) Hartmann layers that develop along the walls which are not parallel to the magnetic field $\mathbf{B}_0$ and of characteristic thickness Ha^{-1}, and 2) parallel layers that develop near walls parallel to $\mathbf{B}_0$ or between two cores which cannot be matched together; these have a characteristic thickness $\mathrm{Ha}^{-1/2}$.

The study of Hartmann layers is required to derive the core solution. Conversely, in many cases of symmetry such as a fully established condition [8. – P. 138 – 146], the parallel layers are passive and can be disregarded since they have no influence on the core flow.

3.1.The core flow solution. In the core (subscript c), neglecting both the Laplacean term and the rot in the right-hand side, equations (13) and (14) become:

$$(\mathbf{e}_B\nabla)\mathbf{m}_c^+ = \mathrm{Ha}\left[\mathbf{J}_{Bc};\mathbf{b}\right]\left\{1+O\left(\mathrm{Ha}^{-1}\right)\right\}, \tag{18}$$

$$(\mathbf{e}_B\nabla)\mathbf{m}_c^- = -\mathrm{Ha}\left[\mathbf{J}_{Bc};\mathbf{b}\right]\left\{1+O\left(\mathrm{Ha}^{-1}\right)\right\}. \tag{19}$$

Let us use a cartesian frame of reference with the z-coordinate in the uniform magnetic field direction (the coordinates x and y will be defined later on). The solutions to equations (18) and (19) are:

$$\mathbf{m}_c^+ = \mathrm{Ha}\int_0^z\left[\mathbf{J}_{Bc};\mathbf{b}\right]dz + \mathbf{m}_2^+(x,y), \tag{20}$$

$$\mathbf{m}_c^- = -\mathrm{Ha}\int_0^z\left[\mathbf{J}_{Bc};\mathbf{b}\right]dz + \mathbf{m}_2^-(x,y), \tag{21}$$

where $\mathbf{m}_2^{\pm}$ are arbitrary functions independent of z.

It is necessary to return to $\mathbf{u}_c$ and $\mathbf{j}_c$ because the boundary conditions cannot be expressed in terms of $\mathbf{m}^+$ and $\mathbf{m}^-$ but in terms of $\mathbf{u}$ and $\mathbf{j}$ Equation (15) gives the current density and equation (8) yields the velocity field:

$$\mathbf{j}_c = \mathbf{j}_{c0} + \mathbf{j}_2(x,y), \quad \mathbf{u}_c = \mathbf{u}_{c0} + z\cdot\mathrm{rot}\left(\mathbf{j}_2(x,y)\right) + \mathbf{u}_2(x,y), \tag{22),(23}$$

where we denote $\mathbf{j}_{c0} = \int_0^z\left[\mathbf{J}_{Bc};\mathbf{b}\right]dz$ and $\mathbf{u}_{c0} = \int_0^z\left\{\left[\mathbf{U}_{Bc};\mathbf{b}\right]+\mathrm{rot}\,\mathbf{j}_{c0}\right\}dz$, two known vector fields depending only on the unperturbed core solution $\mathbf{U}_{Bc}$ and $\mathbf{J}_{Bc}$ and on the non-uniformity of the magnetic field $\mathbf{b}$; and where $\mathbf{u}_2$ and $\mathbf{j}_2$ are arbitrary functions independent of z. Continuity equations for $\mathbf{u}$ and $\mathbf{j}$ (equations (5) and (6)) impose that:

$$\mathrm{div}\,\mathbf{j}_2 = \mathrm{div}\,\mathbf{j}_{c0}, \quad \mathrm{div}\,\mathbf{u}_2 = -(\mathbf{e}_z\mathrm{rot}\,\mathbf{j}_2 + \mathrm{div}\,\mathbf{u}_{c0}). \tag{24),(25}$$

3.2. The Hartmann layers. In these regions whose characteristic thickness is of order Ha^{-1}, the variations in the normal direction are dominant and $\mathbf{e}_B\mathbf{n}\neq 0$ (we denote by $\mathbf{n}$ the normal vector directed into the fluid and n the coordinate in this direction). We extend the core solution to the whole cavity and take the difference between the equations for the actual solution and those for the core solution:

$$\Delta(\mathbf{m}^+ - \mathbf{m}_c^+) - \mathrm{Ha}(\mathbf{e}_B\nabla)(\mathbf{m}^+ - \mathbf{m}_c^+) = \\ = \mathrm{Ha}\left\{\mathrm{rot}\left[\mathbf{U}_B - \mathbf{U}_{Bc};\mathbf{b}\right] + \mathrm{Ha}\left[\mathbf{J}_B - \mathbf{J}_{Bc};\mathbf{b}\right]\right\}, \tag{26}$$

$$\Delta(\mathbf{m}^- - \mathbf{m}_c^-) - \mathrm{Ha}(\mathbf{e}_B\nabla)(\mathbf{m}^- - \mathbf{m}_c^-) = \\ = -\mathrm{Ha}\left\{\mathrm{rot}\left[\mathbf{U}_B - \mathbf{U}_{Bc};\mathbf{b}\right] - \mathrm{Ha}\left[\mathbf{J}_B - \mathbf{J}_{Bc};\mathbf{b}\right]\right\}, \tag{27}$$

$$\mathrm{div}(\mathbf{m}^+ - \mathbf{m}_c^+) = \mathrm{div}(\mathbf{m}^- - \mathbf{m}_c^-) = 0. \tag{28}$$

Using the approximations $\Delta = \partial_n^2$ and $(\mathbf{e}_B\nabla) = (\mathbf{e}_B\mathbf{n})\partial_n$ and writing that

$$\mathrm{rot}\left[\mathbf{U}_B - \mathbf{U}_{Bc};\mathbf{b}\right] = -(\mathbf{b}\nabla)(\mathrm{rot}(\mathbf{U}_B - \mathbf{U}_{Bc}))$$

and

$$\left[\mathbf{J}_B - \mathbf{J}_{Bc};\mathbf{b}\right] = -(\mathbf{b}\nabla)(\mathbf{J}_B - \mathbf{J}_{Bc}),$$

equations (26) and (27) become:

$$(\partial_n^2 + \mathrm{Ha}\cos\theta\,\partial_n)\,(\mathbf{m}^+ - \mathbf{m}_c^+) = -\,\mathrm{Ha}(\mathbf{b}\nabla)(\mathbf{M}_B^+ - \mathbf{M}_{Bc}^+) \tag{29}$$

$$(\partial_n^2 - \mathrm{Ha}\cos\theta\,\partial_n)\,(\mathbf{m}^- - \mathbf{m}_c^-) = \mathrm{Ha}(\mathbf{b}\nabla)(\mathbf{M}_B^- - \mathbf{M}_{Bc}^-), \tag{30}$$

where $\cos\theta = \mathbf{e}_B\mathbf{n}$ characterizes the vector angle between the direction of the uniform magnetic field $\mathbf{e}_B$ and the normal direction $\mathbf{n}$, and $\mathbf{M}_B^{\pm} = \mathrm{rot}\,\mathbf{U}_B \pm \mathrm{Ha}\,\mathbf{J}_B$ denote the known modified Elsasser variables for the unperturbed flow. In the following, we shall term S^- a surface where $\mathbf{e}_B\mathbf{n} = \cos\theta < 0$ and S^+ a surface where $\mathbf{e}_B\mathbf{n} = \cos\theta > 0$. As observed at the begining of this section, it appears that $\mathbf{m}^+$ has no Hartmann layer along surfaces S^- and $\mathbf{m}^-$ has no Hartmann layer along surfaces S^+.

Solutions of (29) and (30) are of the form:

$$\mathbf{m}^{\pm} - \mathbf{m}_c^{\pm} = \mathbf{a}\,\exp\left(-\mathrm{Ha}|\cos\theta|n\right) + \mathbf{p.s.} \tag{31}$$

where **p.s.** is a particular solution, $\mathbf{a}$ is a vector field independent of n, $|\cos\theta| = -\cos\theta$ on S^- and $|\cos\theta| = \cos\theta$ on S^+. We look for simple particular solutions in $\exp(-\mathrm{Ha}|\cos\theta|n)$. Taking $(\mathbf{bn}) = (\mathbf{bn})_{|n=0}$ and supposing further that $(\mathbf{bn})_{|n=0} \neq 0$, we obtain:

$$\mathbf{m}^+ - \mathbf{m}_c^+ = (\mathbf{a}^+ - n\mathrm{Ha}(\mathbf{bn})\mathbf{M}_0^+)\exp\left(-\mathrm{Ha}|\cos\theta|n\right), \tag{32}$$

$$\mathbf{m}^- - \mathbf{m}_c^- = (\mathbf{a}^- + n\mathrm{Ha}(\mathbf{bn})\mathbf{M}_0^-)\exp\left(-\mathrm{Ha}|\cos\theta|n\right), \tag{33}$$

where $\mathbf{M}_0^{\pm}$ is the tangential component of $\mathbf{M}_B^{\pm} - \mathbf{M}_{Bc}^{\pm}$.

Denoting by $\mathbf{m}_0^{\pm}$ the tangential part of $\mathbf{a}^{\pm}$, we get from the equation (15):

$$(\mathbf{j} - \mathbf{j}_c)_t = 1/2\left\{\mathrm{Ha}^{-1}(\mathbf{m}_0^+ - \mathbf{m}_0^-) - n(\mathbf{bn})(\mathbf{M}_0^+ + \mathbf{M}_0^-)\right\}\exp(-\mathrm{Ha}|\cos\theta|n). \tag{34}$$

Using the continuity equation for $\mathbf{m}^{\pm} - \mathbf{m}_c^{\pm}$, we can relate their normal and tangential components; the derivation, carried out in the appendix, yields:

$$(\mathbf{j} - \mathbf{j}_c)_n = \frac{1}{2}\left\{\mathrm{Ha}^{-2}\mathrm{div}\left(\frac{\mathbf{d}_0^+ - \mathbf{d}_0^-}{|\cos\theta|}\right) - n\mathrm{Ha}^{-1}\left[\left(\frac{\mathbf{d}_0^+ - \mathbf{d}_0^-}{|\cos\theta|}\right)\mathrm{grad}|\cos\theta| + \right.\right.$$

$$\left.\left. + \left(\frac{\mathbf{M}_0^+ - \mathbf{M}_0^-}{|\cos\theta|}\right)\mathrm{grad}(\mathbf{bn})\right]\right\}\exp\left(-\mathrm{Ha}|\cos\theta|n\right) - \tag{35}$$

$$-1/2\,n(\mathbf{bn})\left[(\mathbf{M}_B^+ - \mathbf{M}_{Bc}^+)_n + (\mathbf{M}_B^- - \mathbf{M}_{Bc}^-)_n\right],$$

where we denote $\mathbf{d}_0^+ = \mathbf{m}_0^+ - \dfrac{(\mathbf{bn}^+)}{|\cos\theta|}\mathbf{M}_0^+$ and $\mathbf{d}_0^- = \mathbf{m}_0^- + \dfrac{(\mathbf{bn}^-)}{|\cos\theta|}\mathbf{M}_0^-$. It is noticeable that $\mathbf{m}_0^{\pm}$ and $\mathbf{d}_0^{\pm}$, like $\mathbf{M}_0^{\pm}$, are independent of n, equal to zero on $S^{\mp}$ and tangential to $S^{\pm}$.

From Ohm's law (8), we then get for the tangential part of $(\mathbf{u}-\mathbf{u}_c)$:

$$(\mathbf{u}-\mathbf{u}_c)_t = \frac{1}{2}\left\{ \mathrm{Ha}^{-1}\mathbf{n}\times\left(\frac{\mathbf{d}_0^+ + \mathbf{d}_0^-}{|\cos\theta|}\right) - \right.$$
$$\left. -n(\mathbf{bn})\mathbf{n}\times\left(\frac{\mathbf{M}_0^+ - \mathbf{M}_0^-}{|\cos\theta|}\right)\right\}\exp\left(-\mathrm{Ha}|\cos\theta|n\right). \tag{36}$$

Finally, from the continuity equation for $(\mathbf{u}-\mathbf{u}_c)$ we find the normal component:

$$(\mathbf{u}-\mathbf{u}_c)_n = \left\{\frac{\mathrm{Ha}^{-2}}{2}\mathrm{div}\left(\mathbf{n}\times\left(\frac{\mathbf{d}_0^+ + \mathbf{d}_0^-}{|\cos\theta|^2}\right) - (\mathbf{bn})\mathbf{n}\times\left(\frac{\mathbf{M}_0^+ - \mathbf{M}_0^-}{|\cos\theta|^2}\right)\right) + \right.$$
$$+n\frac{\mathrm{Ha}^{-1}}{2}(\mathbf{bn})\left(\mathbf{n}\times\left(\frac{\mathbf{M}_0^+ - \mathbf{M}_0^-}{|\cos\theta|^3}\right)\right)\mathrm{grad}|\cos\theta| -$$
$$-n\left[\frac{\mathrm{Ha}^{-1}}{2}\left(n\times\left(\frac{\mathbf{d}_0^+ + \mathbf{d}_0^-}{|\cos\theta|^2}\right)\right)\mathrm{grad}|\cos\theta| + \frac{\mathrm{Ha}^{-1}}{2}\mathrm{div}\left((\mathbf{bn})\mathbf{n}\times\left(\frac{\mathbf{M}_0^+ - \mathbf{M}_0^-}{|\cos\theta|^2}\right)\right) - \right. \tag{37}$$
$$\left.\left. -n(\mathbf{bn})\left(\mathbf{n}\times\left(\frac{\mathbf{M}_0^+ - \mathbf{M}_0^-}{2|\cos\theta|^2}\right)\right)\mathrm{grad}|\cos\theta|\right]\right\}\exp\left(-\mathrm{Ha}|\cos\theta|n\right).$$

We have now obtained the general form of the current density and velocity in the core ((22) and (23)) and in the Hartmann layers ((34) – (37)). These solutions are expressed in terms of four unknown two-dimensional vectors: $\mathbf{u}_2$, $\mathbf{j}_2$, $\mathbf{m}_0^+$ and $\mathbf{m}_0^-$, and still have to satisfy: the boundary conditions for $\mathbf{u}$ and $\mathbf{j}$, equations (24) and (25) concerning the variables $\mathbf{u}_2$ and $\mathbf{j}_2$ and the tangency conditions concerning the variables $\mathbf{m}_0^+$ and $\mathbf{m}_0^-$. These conditions, whose expressions can only be explicited for a given particular configuration, lead to a system of partial differential equations for the four two-dimensional vectors. In the following section, we propose a derivation of the solution in the case of a horizontal symmetric Bridgman configuration with simple electrical conditions.

4. Solution for a horizontal symmetric Bridgman configuration. Let us now focus on buoyancy-driven convection in a horizontal symmetric Bridgman configuration with a vertical magnetic field. The crucible is a finite length cylinder whose endwalls are maintained at fixed temperature (see Fig. 1). Because the Prandtl number is much smaller than unit, the temperature field may be expressed assuming pure conduction, thus the temperature gradient is uniform: grad $T = G\,\mathbf{e}_x$. The cold wall ($T = T_0$) represents the solidification front that we assume at rest. We consider that the melt is a very

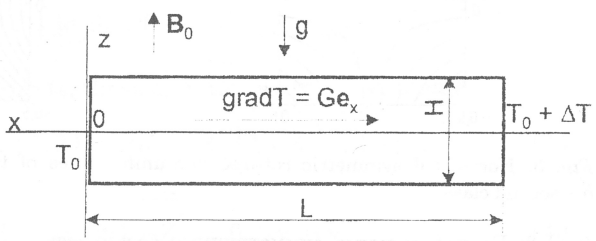

Fig. 1. Problem definition.

Рис. 1. К постановке задачи.

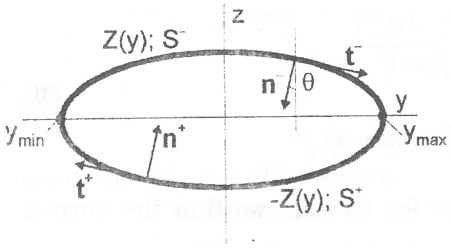

Fig. 2. Scheme of cross-section of the working volume. Curves $Z(y)$ and $-Z(y)$ forming the surfaces S^- and S^+ are indicated.

Рис. 2. Эскиз поперечного сечения рабочего объема. Показаны кривые $Z(y)$ и $-Z(y)$, образующие поверхности S^- и S^+ соответственно.

dilute mixture and that only thermal buoyancy acts as a driving force. We assume the cylinder aspect ratio H/L to be small enough for a fully established flow to exist in the middle.

The reference frame ($\mathbf{e}_x$, $\mathbf{e}_y$, $\mathbf{e}_z$), where $\mathbf{e}_z$, has been defined in section 2, is shown in Figs 1 and 2. We assume that the cylinder is symmetric with respect to $\mathbf{e}_y$, its cross-section shape being defined by the function $Z(y)$ representing its outer contour; this function $Z(y)$ corresponds to a surface S^- ($\mathbf{e}_B\mathbf{n} = \cos\theta < 0$) and the function $-Z(y)$ corresponds to a surface S^+ ($\mathbf{e}_B\mathbf{n} = \cos\theta > 0$) (Fig. 2). And we also assume that the magnetic field disturbance $\mathbf{b}$ is independent of x and has its magnetic flux lines symmetric with respect to $\mathbf{e}_y$. This assumption leads to distinguish two classes of non-uniformities: those with horizontal and vertical pole lines (Fig. 3*a*) and those with pole lines inclined at 45° (Fig. 3*b*). The first class non-uniformity ($\mathbf{b}_1$) satisfies the conditions $b_y(y, z) = b_y(y, -z)$ and $b_z(y, z) = -b_z(y, -z)$, while the second class non-uniformity ($\mathbf{b}_2$) satisfies the conditions $b_y(y, z) = -b_y(y, -z)$ and $b_z(y, z) = b_z(y, -z)$. These rot-free non-uniform fields $\mathbf{b}_1$ and $\mathbf{b}_2$ sketched in Fig. 3 have a linear dependence on y and z.

The vectors $\mathbf{u}_2$ and $\mathbf{j}_2$ are expressed in the ($\mathbf{e}_x$, $\mathbf{e}_y$, $\mathbf{e}_z$) frame of reference while the vectors $\mathbf{m}_0^{\pm}$ and $\mathbf{d}_0^{\pm}$ are expressed in the local frame ($\mathbf{e}_x$, $\mathbf{n}^{\pm}$, $\mathbf{t}^{\pm}$) where the vector $\mathbf{n}$ (resp.$\mathbf{t}$) denotes the unit vector normal (resp.tangential) to the wall. The coordinate transformation from ($\mathbf{e}_y$, $\mathbf{e}_z$) into ($\mathbf{n}^{\pm}$, $\mathbf{t}^{\pm}$) is the same as in [1]. Now, the unperturbed solution ($\mathbf{U}_B$ and $\mathbf{J}_B$) corresponds to the solution derived in [1], and thus the vectors $\mathbf{u}_{c0}$ and $\mathbf{j}_{c0}$ are known. The boundary conditions for $\mathbf{u}$ and $\mathbf{j}$ are: 1) zero-velocity at the walls for the velocity field, and 2) perfectly insulating or perfectly conducting walls for the electrical conditions.

4.1. Electrically perfectly insulating walls. 4.1.1.Derivation of the solution. Expressing $\mathbf{u}=\mathbf{u}_c+(\mathbf{u}-\mathbf{u}_c)$ and $\mathbf{j}=\mathbf{j}_c+(\mathbf{j}-\mathbf{j}_c)$, as given by equations (22), (23) and (34) to (37), which have to satisfy the boundary conditions, we

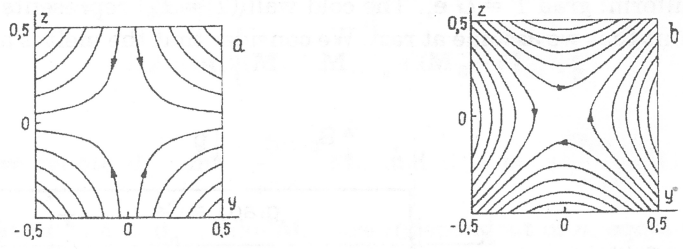

Fig. 3. Horizontal symmetric rot-free non-uniformities of the magnetic field: *a* – first class, *b* – second class.

Рис. 3. Горизонтальные симметричные безвихревые неоднородности магнитного поля первого (*a*) и второго (*b*) классов.

we obtain the system of equations (38) to (43), where prims denote the ∂_y derivatives and where we used the condition of a fully established flow ($\partial_x = 0$).

1) (38^+) and (38^-) express that S^+ and S^- are electrically insulating walls (**jn** = 0 at $n = 0$):

$$Z'\left[j_{2y} + j_{c0y}(-Z)\right] + j_{2x} + j_{c0x}(-Z) - 1/2\,\mathrm{Ha}^{-2}\left[d_{0t}^{+}\sqrt{1+Z'^2}\right]' = 0, \qquad (38^+)$$

$$Z'\left[j_{2y} + j_{c0y}(Z)\right] - j_{2x} - j_{c0x}(Z) - 1/2\,\mathrm{Ha}^{-2}\left[d_{0t}^{-}\sqrt{1+Z'^2}\right]' = 0. \qquad (38^-)$$

2) (39^+), (39^-) and (40^+), (40^-) express the zero tangential velocity condition along $\mathbf{e}_x$ and **t** (**ue**$_x$ = 0 and **ut** = 0 at $n = 0$):

$$u_{2x} + u_{c0x}(-Z) - Zj'_{2x} + 1/2\,\mathrm{Ha}^{-1}\left[d_{0t}^{+}\sqrt{1+Z'^2}\right] = 0, \qquad (39^+)$$

$$u_{2x} + u_{c0x}(Z) + Zj'_{2x} + 1/2\,\mathrm{Ha}^{-1}\left[d_{0t}^{-}\sqrt{1+Z'^2}\right] = 0, \qquad (39^-)$$

$$-u_{2y} + Z\,Z'\,j'_{2x} + Z'u_{2z} - 1/2\,\mathrm{Ha}^{-1}\left[d_{0x}^{+}\left(1+Z'^2\right)\right] = 0, \qquad (40^+)$$

$$u_{2y} - Z\,Z'\,j'_{2x} + Z'u_{2z} - 1/2\,\mathrm{Ha}^{-1}\left[d_{0x}^{-}\left(1+Z'^2\right)\right] = 0. \qquad (40^-)$$

3) (41^+) and (41^-) express the non-penetrability condition for the walls S^+ and S^- (**un** = 0 at $n = 0$):

$$Z'u_{2y} + Zj'_{2x} + u_{2z} + 1/2\,\mathrm{Ha}^{-2}\left[d_{0x}^{+}\sqrt{1+Z'^2}\right]' = 0, \qquad (41^+)$$

$$Z'u_{2y} + Zj'_{2x} - u_{2z} - 1/2\,\mathrm{Ha}^{-2}\left[d_{0x}^{-}\sqrt{1+Z'^2}\right]' = 0 \qquad (41^-)$$

4) (42) and (43) express (24) and (25) in terms of vector components:

$$j'_{2y} = -\mathrm{div}\,\mathbf{j}_{c0} \text{ or, equivalently, } j_{2y} = \int_0^y -\mathrm{div}\,\mathbf{j}_{c0}\,dy + k_{2y}, \qquad (42)$$

$$u'_{2y} = j'_{2x}. \qquad (43)$$

We still have to write the conditions of zero mass and electric current fluxes in the x and y directions; since the ends of the cavity are closed with insulating and impermeable walls, we have:

$$\int_{y_{min}}^{y_{max}}\int_{-Z}^{Z} \mathbf{ue}_x\,dz\,dy = 0\ ; \quad \int_{y_{min}}^{y_{max}}\int_{-Z}^{Z} \mathbf{je}_x\,dz\,dy = 0.$$

And since there are no line of sources or sinks of mass or electric current along the walls, we also have:

$$\int_{-Z}^{Z} \mathbf{ue}_y\,dz = 0\ ; \quad \int_{-Z}^{Z} \mathbf{je}_y\,dz = 0 \quad \forall y \in \left[y_{min}; y_{max}\right].$$

In terms of vector components, these equations can be written as:

$$\int_{y_{min}}^{y_{max}} \left\{ 2Zu_{2x} + \int_{-Z}^{Z} u_{c0x}\,dz + 1/2\,\mathrm{Ha}^{-2}\left[d_{0t}^{+} - d_{0t}^{-}\right]\left(1+Z'^2\right)\right\} dy = 0, \qquad (44)$$

$$2Zu_{2y} + 1/2\,\mathrm{Ha}^{-2}\left[d_{0x}^{+} - d_{0x}^{-}\right]\sqrt{1+Z'^2} = 0 \quad \forall y \in \left[y_{min}; y_{max}\right], \qquad (45)$$

$$\int_{y_{\min}}^{y_{\max}} \left\{ 2Zj_{2x} + 1/2\,\mathrm{Ha}^{-2}\left[d_{0x}^{+} - d_{0x}^{-}\right]\sqrt{1+Z'^{2}} \right\} \mathrm{d}y = 0, \tag{46}$$

$$\int_{-Z}^{Z} (j_{c0y} + j_{2y})\mathrm{d}z - 1/2\,\mathrm{Ha}^{-2}\left[d_{0t}^{+} - d_{0t}^{-}\right]\sqrt{1+Z'^{2}} = 0;\ \forall y \in \left[y_{\min}; y_{\max}\right]. \tag{47}$$

The system of equations (38) – (47) is similar to the system obtained in [1] and can be solved in the same way. The subsystem (40), (41), (43), (45) and (46) yields the partial solution:

$$d_{0x}^{+} = d_{0x}^{-} = u_{2y} = u_{2z} = j_{2x} = 0\,. \tag{48}$$

Let us substitute d_{0t}^{+} and d_{0t}^{-} in (38) from (39). The combination (38^{+})–(38^{-}) yields

$$j_{2z} = 1/2\left\{ Z'\left(j_{c0y}(Z) - j_{c0y}(-Z)\right) - j_{c0z}(Z) - j_{c0z}(-Z) \right\}. \tag{49}$$

Let us substitute d_{0t}^{+} and d_{0t}^{-} in (47) from (39); we get an integral form of the combination (38^{+}) and (38^{-}) that leads to

$$u_{2x} = \mathrm{Ha}\left\{ -Zj_{2y} - \frac{1}{2}\int_{-Z}^{Z} j_{c0y}\mathrm{d}z \right\}. \tag{50}$$

Then, substituing u_{2x} in (42) from (50), with (44), we get

$$j_{2y} = \int_{0}^{y} -\mathrm{div}\mathbf{j}_{c0}\mathrm{d}y + \int_{y_{\min}}^{y_{\max}} Z\left\{ -\int_{-Z}^{Z} j_{c0y}\mathrm{d}z + 2Z\int_{0}^{y} \mathrm{div}\mathbf{j}_{c0}\mathrm{d}\eta \right\}\mathrm{d}y \Big/ \int_{y_{\min}}^{y_{\max}} 2Z^{2}\mathrm{d}y\,. \tag{51}$$

The core solution is now complete. The solution in the Hartmann layers can be easily derived from (39): velocity and normal component of the current density both decrease exponentially in order to reach zero values at the walls.

Table 1

The way how the class of symmetry of the magnetic non-uniformity **b** determines the order of magnitude of the perturbations in the core

b	**1st class of symmetry** (horizontal and vertical pole lines)		**2nd class of symmetry** (45° inclined pole lines)	
variable	order of magnitude	class of symmetry or parity with respect to z	order of magnitude	class of symmetry or parity with respect to z
$\mathbf{J}_B$	$\mathrm{Gr/Ha^2}$	2nd class	$\mathrm{Gr/Ha^2}$	2nd class
$\mathbf{U}_B$	$\mathrm{Gr/Ha^2}$	odd	$\mathrm{Gr/Ha^2}$	odd
$[\mathbf{J}_B; \mathbf{b}]$	$\lambda\mathrm{Gr/Ha^2}$	2nd class	$\lambda\mathrm{Gr/Ha^2}$	1st class
$[\mathbf{U}_B; \mathbf{b}]$	$\lambda\mathrm{Gr/Ha^2}$	odd	$\lambda\mathrm{Gr/Ha^2}$	even
$\mathbf{j}_{c0}$	$\lambda\mathrm{Gr/Ha^2}$	1st class	$\lambda\mathrm{Gr/Ha^2}$	2nd class
$\mathrm{div}\,\mathbf{j}_{c0}$	$\lambda\mathrm{Gr/Ha^2}$		$=0$	
$\mathbf{u}_{c0}$	$\lambda\mathrm{Gr/Ha^2}$	even	$\lambda\mathrm{Gr/Ha^2}$	odd
$\mathbf{j}_{2z}$	$=0$		$\lambda\mathrm{Gr/Ha^2}$	
$\mathbf{j}_{2y}$	$\lambda\mathrm{Gr/Ha^2}$		$=0$	
$\mathbf{u}_{2x}$	$\lambda\mathrm{Gr/Ha}$		$=0$	
$\mathbf{j}_c$	$\lambda\mathrm{Gr/Ha^2}$	1st class	$\lambda\mathrm{Gr/Ha^2}$	2nd class
$\mathbf{u}_c$	$\lambda\mathrm{Gr/Ha}$	even	$\lambda\mathrm{Gr/Ha^2}$	odd

From equations (50) and (51), we deduce that it is not only the order of magnitude of the vector $\mathbf{j}_{c0}$ that determines the order of magnitude of the variable u_{2x}, but also its class of symmetry. The non-uniformity $\mathbf{b}$ does not appear directly in the solution but is included in the definition of

$$\mathbf{j}_{c0} = \int_0^z [\mathbf{J}_{Bc}; \mathbf{b}]\, dz = -\int_0^z \mathrm{rot}(\mathbf{J}_{Bc} \times \mathbf{b})\, dz\,,$$

that appears in the expressions of the variables. Thus, knowing that the unperturbed current density in the core $\mathbf{J}_{Bc}$ has the same symmetry as $\mathbf{b}_2$, it is finally the class of symmetry of the non-uniformity $\mathbf{b}$ which determines the order of magnitude of the velocity perturbation in the core. The Table 1 gives the order of magnitude, class of symmetry or parity with respect to z of the different variables, and illustrates how the class of symmetry of $\mathbf{b}$ determines the order of magnitude of the perturbations: 1) if $\mathbf{b}$ has inclined pole lines, the velocity perturbation in the core is of order $\lambda \mathrm{GrHa}^{-2}$, 2) if $\mathbf{b}$ has horizontal and vertical pole lines, the velocity perturbation is of order $\lambda \mathrm{GrHa}^{-1}$, and 3) in all cases, the perturbation of the current density in the core is of the order $\lambda \mathrm{GrHa}^{-2}$.

4.1.2. Some illustrations. In order to illustrate the results of the previous paragraph, let us focus on the two particular linear non-uniformities $\mathbf{b}_1$ and $\mathbf{b}_2$ introduced at the begining of this section. Figs 4 – 6 present the core solutions for three cross-sectional shapes.

Some characteristic features are noticeable:

1) For a circular cross-section (Fig. 4) and the second-class magnetic field non-uniformity $\mathbf{b}_2$, the core velocity perturbation is of order $\lambda \mathrm{GrHa}^{-2}$, varies in the y- and z-directions, and has the same symmetry as $\mathbf{b}_2$. The electric current is mainly in the z-direction. The electric current lines close naturally in the fluid, so that the Hartmann layers are passive. With the first class non-uniformity $\mathbf{b}_1$, the current flux is mainly in the y-direction. The y-component of the current density in the core, j_{cy}, is an even function of z and for most values of y, the y-component of the electric current flux is non-zero and scales with $\lambda \mathrm{GrHa}^{-2}$. An opposite current flux must then flow in the Hartmann layers. Furthermore, we know that the current in the Hartmann layers is proportional to the core velocity [8.– P. 150–164]. The characteristic thickness of

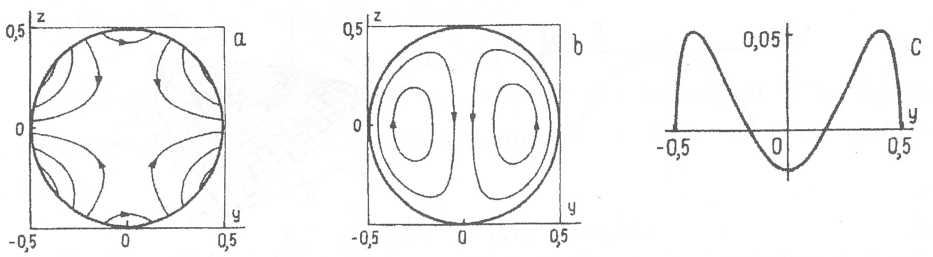

Fig. 4. Perturbations in the core for the circular cross-section with insulating walls. Electric current lines with the 1st class non-uniformity $\mathbf{b}_1$ (*a*), with the 2nd class non-niformity $\mathbf{b}_2$ (*b*); velocity profile ($u_c \sim \lambda \mathrm{Gr/Ha}$) along the axis z=0 at the 1st class non-uniformity $\mathbf{b}_1$ (*c*).

Рис. 4. Возмущения в ядре течения при круглом поперечном сечении рабочего объема и непроводящих стенках: линии плотности электрического тока при неоднородностях первого ($\mathbf{b}_1$; *a*) и второго ($\mathbf{b}_2$; *b*) классов; профиль скорости $u_c \sim \lambda \mathrm{Gr/Ha}$ вдоль оси $z = 0$ при неоднородности первого класса $\mathbf{b}_1$ (*c*).

the Hartmann layers being Ha^{-1} and the current flux in this layers scaling with $\lambda GrHa^{-2}$, the current scales with $\lambda GrHa^{-1}$, and so does the velocity perturbation.

2)For a square cross-section (Fig. 5) and $\mathbf{b}_2$, the velocity field and electric current lines behave like as at a circular cross-section. But for the case of $\mathbf{b}_1$, though j_{cy} is an even function of z, for and y, the y-flux component is zero and so the Hartmann layers are passive. The velocity could thus be expected to scale with $\lambda GrHa^{-2}$.

3) Now, for the 45° inclined square cross-section (Fig. 6) and first class non-uniformity $\mathbf{b}_1$, we observe the same behaviour as for the circular cross-section, too. On the other hand, for the $\mathbf{b}_2$ second class non-uniformity, we find a zero velocity perturbation; it is interesting to recall that the zeroth order velocity $\mathbf{U}_{Bc}$ was zero, too.

4) There exist parallel layers for a square cross-section (on both sides $y = \pm 0{,}5$, see Fig. 5) and for a 45° inclined square cross-section (along the line $y = 0$, see Fig. 6). These layers accomodate jumps in the electric current and electric potential between the core and the wall or between the two cores. Our study does not predict anything concerning these layers.

4.2. Perfectly conducting walls. 4.2.1. Derivation of the solution. The only difference from the insulating case is the electrical condition at the walls, $\mathbf{j}\times\mathbf{n} = 0$ at $n = 0$ (instead of $\mathbf{jn} = 0$). In the system (38) – (43), Eq. (38) is replaced by Eq. (52) and (53) which express the condition of zero tangential part of the electric current along $\mathbf{t}$ and $\mathbf{e}_x$ at the walls S^+ and S^-:

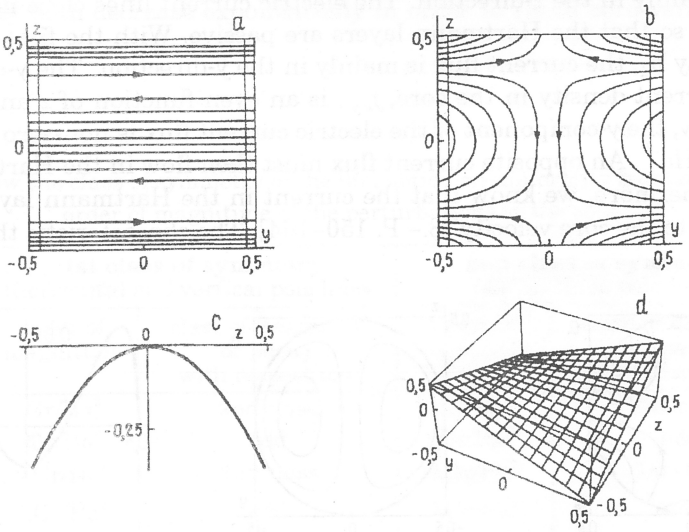

Fig. 5. Perturbations in the core for the square cross-section with insulating walls. Electric current lines with the 1st class non-uniformity $\mathbf{b}_1$ (*a*), with the 2nd class non-uniformity $\mathbf{b}_2$ (*b*); velocity profile ($u_c \sim \lambda Gr/Ha^2$) along $y = 0$ with the 1st class non-uniformity $\mathbf{b}_1$ (*c*); velocity ($u_c \sim \lambda Gr/Ha^2$) with the 2nd class non-uniformity $\mathbf{b}_2$ (*d*).

Рис. 5. Возмущения в ядре течения при квадратном поперечном сечении рабочего объема и непроводящих стенках: линии плотности электрического тока при неоднородностях первого ($\mathbf{b}_1$; *a*) и второго ($\mathbf{b}_2$; *b*) классов; профиль скорости $u_c \sim \lambda Gr/Ha^2$ вдоль оси $y = 0$ при неоднородности первого класса $\mathbf{b}_1$ (*c*) и скорость $u_c \sim \lambda Gr/Ha^2$ при неоднородности второго класса $\mathbf{b}_2$ (*d*).

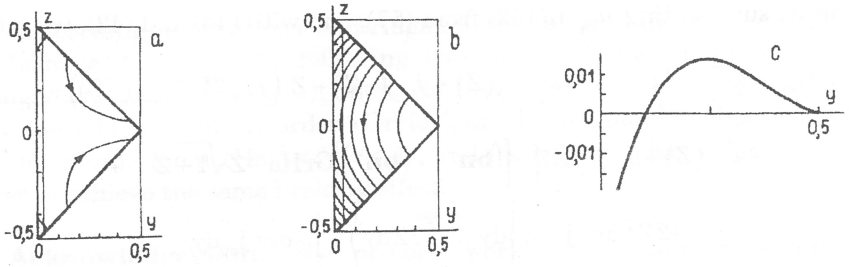

Fig. 6. Perturbations in the core for the 45° inclined square cross-section with insulating walls. Eelectric current lines with the 1st class non-uniformity $\mathbf{b}_1$ (a), with the 2nd class non-uniformity $\mathbf{b}_2$ (b); velocity profile ($u_c \sim \lambda \mathrm{Gr/Ha}$) along the axis $z = 0$ at the 1st class non-uniformity $\mathbf{b}_1$ (c).

Рис. 6. Возмущения в ядре течения при наклонном под углом 45° квадратном поперечном сечении рабочего объема и неоднородностях первого ($\mathbf{b}_1$; a) и второго ($\mathbf{b}_2$; b) классов; профиль скорости $u_c \sim \lambda \mathrm{Gr/Ha}$ вдоль оси $z = 0$ при неоднородности первого класса $\mathbf{b}_1$ (c).

$$j_{2y} + j_{c0y}(-Z) - Z'\left[j_{2z} + j_{c0z}(-Z)\right] - 1/2\,\mathrm{Ha}^{-1}\left[m_{0t}^{+}\sqrt{1+Z'^{2}}\right] = 0, \qquad (52^{+})$$

$$-j_{2y} - j_{c0y}(Z) - Z'\left[j_{2z} + j_{c0z}(Z)\right] - 1/2\,\mathrm{Ha}^{-1}\left[m_{0t}^{-}\sqrt{1+Z'^{2}}\right] = 0, \qquad (52^{-})$$

$$j_{2x} + 1/2\,\mathrm{Ha}^{-1} m_{0x}^{+} = 0, \quad j_{2x} - 1/2\,\mathrm{Ha}^{-1} m_{0x}^{-} = 0. \qquad (53^{+}),(53^{-})$$

The electric charge conservation equations (46) and (47) are not valid here, because the electric current can freely circulate in the walls. Nevertheless, we must specify the way the two surfaces S^{+} and S^{-} are electrically connected. We here assume that they are in contact, so, they have the same electric potential. This condition is obtained projecting Ohm's law (9) along $\mathbf{e}_z$ and integrating between $-Z$ and Z (using equation (22)):

$$2Zj_{2z} + \int_{-Z}^{Z} j_{c0z}\,dz + \int_{-Z}^{Z} (\mathbf{U}_B \times \mathbf{b})\mathbf{e}_z\,dz. \qquad (54)$$

Like as for the insulating case, our system of equations is similar to the one obtained in [1] and can be solved in the same manner. The subsystem of equations (53), (40), (41), (43), (45) gives

$$d_{0x}^{+} = d_{0x}^{-} = u_{2y} = u_{2z} = j_{2x} = 0\,. \qquad (55)$$

Let us substitute m_{0t}^{+} and m_{0t}^{-} in (52) with the help of (39), M_{0t}^{+} and M_{0t}^{-} being known from [1]. The combination of (52^{+}) and (52^{-}), and (54) yields

$$j_{2z} = \frac{1}{2Z}\int_{-Z}^{Z}\left\{-j_{c0z} + (\mathbf{U}_B \times \mathbf{b})\mathbf{e}_z\right\}dz. \qquad (56)$$

The combination $(52^{+}) - (52^{-})$ gives

$$u_{2x} = -j_{2y} - 1/2\Big\{j_{c0y}(Z) + j_{c0y}(-Z) + Z'\left(j_{c0z}(Z) - j_{c0z}(-Z)\right) + \\ + u_{c0x}(Z) + u_{c0x}(-Z)\Big\} + 1/2\left[(\mathbf{bn}^{-}) + (\mathbf{bn}^{+})\right]\mathrm{GrHa}^{-2} Z\sqrt{1+Z'^{2}}\,. \qquad (57)$$

Finally, substituting u_{2x} in (52) from (57), and with (44) and (42), we get

$$j_{2y} = \left\langle \int_{y_{\min}}^{y_{\max}} \left\{ \int_{-Z}^{Z} u_{c0x} dz - Z\left[j_{c0y}(Z) + j_{c0y}(-Z) + Z'\left(j_{c0z}(Z) - j_{c0z}(-Z) \right) + \right.\right.\right.$$
$$+ u_{c0x}(Z) + u_{c0x}(-Z) \Big] - \Big[\left(\mathbf{bn}^-\right) + \left(\mathbf{bn}^+\right) \Big] \mathrm{GrHa}^{-2} Z \sqrt{1 + Z'^2} + \qquad (58)$$
$$\left.\left.\left. + 2Z \int_0^y \operatorname{div} \mathbf{j}_{c0} dy \right\} dy \Big/ \int_{y_{\min}}^{y_{\max}} 2Z dy \right\rangle + \int_0^y -\operatorname{div} \mathbf{j}_{c0} dy.$$

The core solution is complete, and the solution for the Hartmann layers can be easily derived from (39); the velocity and the tangential component of the current density both decrease exponentially in order to reach zero value at the walls. From equations (56), (57) and (58), it appears that u_{2x}, j_{2y} and j_{2z} are of the same order of magnitude, $\lambda \mathrm{GrHa}^{-2}$. For any non-uniformity **b**, the velocity perturbation and current density in the core scale with $\lambda \mathrm{GrHa}^{-2}$.

5. Conclusions. In this work, the velocity and current density perturbations **u** and **j** due to a slight non-uniformity of the magnetic field **b** superposed to the uniform magnetic field $\mathbf{B}_0$ are determined. This result is applied to get some answer about the required uniformity for the magnetic field in the horizontal Bridgman process.

The formulation and solutions of the problem in sections 2 and 3 are general, since we only assume that the flow in a uniform magnetic field has been determined. The modified Elsasser variables, $\mathbf{m}^+$ and $\mathbf{m}^-$, are useful to solve the problem, but the solution in the Hartmann layers involved more tedious algebra than in [1] because the right-hand sides of (24) and (25) contain a source term related to the interaction of the zeroth order solution and the non-uniformity. The return to the variables **u** and **j** is not simple either. Then, in section 4, in order to complete the derivation of the solution, we focus on buoyancy-driven convection in a typical Bridgman process. We study a symmetric configuration: cross-section and magnetic non-uniformity are symmetric with respect to the horizontal direction. We also suppose that the magnetic non-uniformity is independent of x. This assumption can seem unrealistic but is necessary for a fully established flow. Finally, the system for the variables $\mathbf{u}_2$, $\mathbf{j}_2$, $\mathbf{m}_0^+$ and $\mathbf{m}_0^-$, is similar to the one obtained in [1], thus, we only give an outline of the solution and focus on the results.

The most striking result in section 4 concerns the case of electrically insulating walls: it appears that the symmetry of the magnetic field non-uniformity determines the order of magnitude of the velocity perturbation in the core. For a non-uniformity with inclined pole lines, it scales with $\lambda \mathrm{GrHa}^{-2}$ while it scales with $\lambda \mathrm{GrHa}^{-1}$ for a non-uniformity with horizontal and vertical pole lines (of course, when the perturbation u_c scales with $\lambda \mathrm{GrHa}^{-1}$, the hypothesis $u/U << 1$ requires that $\lambda \mathrm{Ha} << 1$). The electric current distribution helps to understand such a difference: in the first case the Hartmann layers are passive and do not interact with the core, whereas in the other case the Hartmann layers are active. There is a net current inside them, and therefore a velocity proportional to this current is driven in the neighbouring core. In the case of perfectly conducting walls, the velocity perturbation scales with $\lambda \mathrm{GrHa}^{-2}$ for any non-uniformity. But apart from symmetry considerations, the key-result is that the existence of a magnetic non-uniformity can entail an Ha-amplified modification of the velocity in the case of insulating crucibles.

Concerning applications to Bridgman crystal growth, this paper gives the furnace designers the following choice. Either the magnetic field is strongly uniform ($\lambda \mathrm{Ha} << 1$); then, its intensity has not to be very large since the velocity is of the order $\lambda \mathrm{Gr}\mathrm{Ha}^{-2}$; or, the magnetic field does not follow this requirement ($\mathrm{Ha}^{-1} < \lambda << 1$), and its intensity has to be Ha times larger to achieve the same braking effect.

Acknowledgement. The present work was conducted within the framework of the GRAMME agreement between the CNES and the CEA.

Appendix. *Solution for the Hartmann layers.* We derive here the solution of the Eqs (26) and (27). The treatment is similar for the two equations, and we focus on Eq. (26). We showed that the solution of (26) is of the form:

$$\mathbf{m}^+ - \mathbf{m}_c^+ = \mathbf{a}\exp\left(-\mathrm{Ha}|\cos\theta|n\right) - n\mathrm{Ha}(\mathbf{bn})\left(\mathbf{M}_0^+\exp\left(-\mathrm{Ha}|\cos\theta|n\right)\right). \tag{32}$$

We write now the continuity equation for $\mathbf{m}^+ - \mathbf{m}_c^+$:

$$\mathrm{div}_t(\mathbf{m}^+ - \mathbf{m}_c^+)_t + \partial_n(m^+ - m_c^+)_n = 0\,. \tag{a-1}$$

This equation implies that the normal component of $\mathbf{m}^+ - \mathbf{m}_c^+$ is Ha times weaker than its tangential one. We separate the normal and tangential component:

$$\begin{aligned}\mathbf{m}^+ - \mathbf{m}_c^+ &= \mathbf{k}\exp\left(-\mathrm{Ha}|\cos\theta|n\right) = \\ &= \left(\mathbf{m}_0^+ - n\mathrm{Ha}(\mathbf{bn})\mathbf{M}_0^+\right)\exp\left(-\mathrm{Ha}|\cos\theta|n\right) + k_n\mathbf{n}\exp\left(-\mathrm{Ha}|\cos\theta|n\right),\end{aligned} \tag{a-2}$$

where 1) $\mathbf{m}_0^+$, is independent of n, equal to zero on S^- and tangential to S^+; 2) k_n, the normal component, is independent of n, and 3) k_t, the tangential component, is linear with n.

Equation (a-1) becomes

$$\mathrm{div}_t\,\mathbf{k}_t - \mathrm{Ha}(\cos\theta)k_n - n\mathrm{Ha}\left(\mathbf{k}_t\mathrm{grad}(\cos\theta)\right) = 0\,. \tag{a-3}$$

Since the different terms of Eq. (a-3) are of the same order of magnitude, Eq. (a-1) cannot be verified when $\cos\theta$ varies. Thus, the normal component k_n cannot be n-independent.

This occurs because we neglected the tangential derivatives in Eq. (26). But the neglected terms may be linear with n and thus of the same order of magnitude as the normal component. In order to take into account these neglected terms, we have to admit a variation with n for the normal component. Let us rewrite (a-1) with k_n being n-dependent. In order to simplify the equation, we take

$$\mathbf{k} = \kappa - n\mathrm{Ha}(\mathbf{bn})\mathbf{K}_B\,, \tag{a-4}$$

where $\mathbf{K}_B$ is defined by the relation $\mathbf{M}_B^+ - \mathbf{M}_{Bc}^+ = \mathbf{K}_B\exp\left(-\mathrm{Ha}|\cos\theta|n\right)$. We obtain a differential equation for κ_n:

$$\begin{aligned}\partial_n\kappa_n - \mathrm{Ha}(\cos\theta)\kappa_n &= -\mathrm{div}\,\mathbf{m}_0^+ + (\mathbf{bn})\mathrm{div}\left(\mathbf{M}_0^+\cos^{-1}\theta\right) + n\mathrm{Ha}\left(\mathbf{m}_0^+\mathrm{grad}(\cos\theta)\right) - \\ &\quad - n\mathrm{Ha}(\mathbf{bn})\mathbf{M}_0^+\cos^{-1}\theta\,\mathrm{grad}(\cos\theta) + n\mathrm{Ha}\left(\mathbf{M}_0^+\mathrm{grad}(\mathbf{bn})\right) = \\ &= -\mathrm{div}\,\mathbf{d}_0^+ - \mathbf{M}_0^+\cos^{-1}\theta\,\mathrm{grad}(\mathbf{bn}) + n\mathrm{Ha}\left\{\mathbf{d}_0^+\mathrm{grad}(\cos\theta) + \mathbf{M}_0^+\mathrm{grad}(\mathbf{bn})\right\}.\end{aligned} \tag{a-5}$$

The notation $\mathbf{d}_0^+ = \mathbf{m}_0^+ - (\mathbf{bn})\mathbf{M}_0^+\cos^{-1}\theta$ allows to obtain a simpler expression for the right-hand side. We see that $\mathbf{d}_0^+$, like $\mathbf{m}_0^+$, is independent of n, is equal to zero on S^- and tangential to S^+. We solve (a-5) and find a linear solution:

$$\kappa_n = \mathrm{Ha}^{-1}\mathrm{div}\left(\mathbf{d}_0^+\cos^{-1}\theta\right) - n\left\{\mathbf{d}_0^+\cos^{-1}\theta\,\mathrm{grad}(\cos\theta) + \mathbf{M}_0^+\cos^{-1}\theta\,\mathrm{grad}(\mathbf{bn})\right\}. \quad \text{(a-6)}$$

Let us now return to $\mathbf{m}^+ - \mathbf{m}_c^+$ using Eq. (a-4):

$$(\mathbf{m}^+ - \mathbf{m}_c^+)_n = \left\{\mathrm{Ha}^{-1}\mathrm{div}\left(\mathbf{d}_0^+\cos^{-1}\theta\right) - n\mathbf{d}_0^+\cos^{-1}\theta\,\mathrm{grad}(\cos\theta) - \right.$$
$$\left. -n\mathbf{M}_0^+\cos^{-1}\theta\,\mathrm{grad}(\mathbf{bn})\right\}\exp\left(-\mathrm{Ha}|\cos\theta|n\right) - n\mathrm{Ha}(\mathbf{bn})(\mathbf{M}_B^+ - \mathbf{M}_{Bc}^+)_n. \quad \text{(a-7)}$$

The solution of Eq. (26) is now complete. Here, $\mathbf{m}^+ - \mathbf{m}_c^+$ is a function of the unknown variable $\mathbf{m}_0^+$ (n-independent, equal to zero on S^- and tangential to S^+) and of the known variable $\mathbf{M}_0^+$ defined in [1]:

$$(\mathbf{m}^+ - \mathbf{m}_c^+)_t = (\mathbf{m}_0^+ - n\mathrm{Ha}(\mathbf{bn})\mathbf{M}_0^+)\exp\left(-\mathrm{Ha}|\cos\theta|n\right), \quad \text{(a-8)}$$

$$(\mathbf{m}^+ - \mathbf{m}_c^+)_n = \left\{\mathrm{Ha}^{-1}\mathrm{div}\left(\mathbf{d}_0^+\cos^{-1}\theta\right) - n\mathbf{d}_0^+\cos^{-1}\theta\,\mathrm{grad}(\cos\theta) - \right.$$
$$\left. -n\mathbf{M}_0^+\cos^{-1}\theta\,\mathrm{grad}(\mathbf{bn})\right\}\exp\left(-\mathrm{Ha}|\cos\theta|n\right) - n\mathrm{Ha}(\mathbf{bn})(\mathbf{M}_B^+ - \mathbf{M}_{Bc}^+)_n. \quad \text{(a-9)}$$

REFERENCES

1. *Alboussiure T., Garandet J.P., Moreau R.* Buoyancy driven convection with a transverse magnetic field. Pt 1. Asymptotic analysis // J. Fluid Mech. – 1993. – Vol. 253. – P. 545–563.

2. *Langlois W.E.* Buoyancy driven flows in crystal growth melts // Ann. Rev. Fluid Mech. – 1985. – Vol. 17. – P. 191–215.

3. *Oreper G.M., Szekely J.* The effect of a magnetic field on transport phenomena in a Bridgman-Stockbarger crystal growth // J. Cryst. Growth. – 1984. – Vol. 67. – P. 405–419.

4. *Vives C., Perry C.* Effects of magnetically damped convection during the controlled solidification of metals and alloys // Int. J. Heat Mass Transfer. – 1987. – Vol. 30. – P. 479–496.

5. *Matthiesen D.H., Wargo M.J., Motakef S., Carlson D.J., Nakos J.S., Witt A.F.* Dopant segregation during vertical Bridgman-Stockbarger growth with melt stabilization by strong axial magnetic fields // J. Cryst. Growth. – 1987. – Vol. 85. – P. 557–560.

6. *Garandet J.P.* On the problem of radial segregation in an idealized Bridgman configuration: scaling and numerical approaches // J. Cryst. Growth. – 1991. – Vol. 114. – P. 593–602.

7. *Garandet J.P., Alboussiure T., Moreau R.* Buoyancy driven convection in a rectangular enclosure with a transverse magentic field // Int. J. Heat Mass Transfer. – 1992. – Vol. 35. – P. 741–748.

8. *Moreau R.* 1990 Magnetohydrodynamics. Kluwer Acad. Publ. – 313 p.

9. *Куликовский А.Г.* О медленных стационарных течениях проводящей жидкости при больших числах Гартмана // Изв. АН СССР. Мех. жидк. и газа. – 1968. – Т. 3, №2. – Р. 3–10.

10. *Todd L.* Magnetohydrodynamic flow along cylindrical pipes under non-uniform transverse magnetic fields // J. Fluid Mech. – 1968. – Vol. 31. – P. 321–342.

11. *Alemany A., Moreau R.* Ecoulement MHD en présence d'un champ magnétique transversal à plusieurs paires de poles // J. de Mécanique. – 1979. – Vol. 18-1. – P. 103–118.

12. *Series R.W., Hurle D.J.T.* The use of magnetic fields in semi-conductor crystal growth // J. Cryst. Growth. – 1991. – Vol. 113. – P. 305–328.

13. *Hirata H., Hoshikawa K.* Silicon crystal growth in a cusp magnetic field // J. Cryst. Growth. – 1989. – Vol. 96. – P. 747–755.

14. *Hirata H., Hoshikawa K.* Three-dimensional numerical analysis of the effects of a cusp magnetic field on the flows, oxygen transport and heat transfer in a Czochralsky silicon melt // J. Cryst. Growth. – 1992. – Vol. 125. – P. 181–207.

15. *Shercliff J.A.* Steady motion of conducting fluids in pipes under transverse magnetic fields // Proc. Camb. Phil. Soc. – 1953. – Vol. 49. – P. 136–144.

Поступила в редакцию 16.11.94